Call: H2020-SC5-2014-two-stage

Topic: SC5-01-2014

PRIMAVERA

Grant Agreement 641727

PRocess-based climate sIMulation: AdVances in high resolution modelling and European climate Risk Assessment

Deliverable D3.1

Quantification of robustness of aerosol-radiation-cloud interactions across models and resolution

Deliverable Title	Quantification of robustness of aerosol-radiation-cloud interactions across models and resolution	
Brief Description	Simulations with models of varying horizontal resolutions and different complexities of representation of cloud and aerosol are compared to identify the aspects that are most robust to resolution and complexity changes.	
WP number	WP3a	
Lead Beneficiary	*Nicolas Bellouin, University of Reading*	
Contributors	*Gill Thornhill, University of Reading* *Annica Ekman, Stockholm University* *Eva Nygren, Stockholm University* *Manu Thomas, Swedish Meteorological and Hydrological Institute* *Torben Koenigk, Swedish Meteorological and Hydrological Institute* *Klaus Wyser, Swedish Meteorological and Hydrological Institute* *Daniel McCoy, University of Leeds* *Paul Field, University of Leeds*	
Creation Date Version Number Version Date	22 Oct. 18 1 22 Oct. 18	
Deliverable Due Date Actual Delivery Date	31 Oct. 18 6 Nov. 18	
Nature of the Deliverable	X	*R - Report*
		P - Prototype
		D - Demonstrator
		O - Other
Dissemination Level/ Audience	X	*PU - Public*
		PP - Restricted to other programme participants, including the Commission services
		RE - Restricted to a group specified by the consortium, including the Commission services
		CO - Confidential, only for members of the consortium, including the Commission services

Version	**Date**	**Modified by**	**Comments**
1.0	22/10/18	Nicolas Bellouin	Original version
1.1	06/11/18	Nicolas Bellouin	Response to comments by Cath Senior (Met Office)

Table of Contents

List of Tables

List of Figures

1. Executive Summary

PRIMAVERA Work Package 3a aimed at quantifying the robustness of radiative fluxes, clouds, and aerosol-cloud interactions across models of different horizontal resolutions and with representations of clouds and aerosols of varying complexity. The focus has been on aerosols and clouds. Aerosols are important for climate because a sizeable fraction of aerosols are emitted by human activities, and because aerosols modify the Earth's radiative budget. Clouds strongly contribute to the radiative budget of the Earth, so simulating their coverage and water content with fidelity is an important feature of a climate model.

Different combinations of resolution and complexity have been sampled. The main conclusions are:

- The sensitivity of aerosol radiative effects to the complexity of aerosol representations depends on the mechanism. Interactions between aerosols and radiation interactions are not sensitive and simple prescriptions reproduce the radiative effects of complex models very well. In contrast, simple prescriptions of interactions between aerosol and clouds need to account for temporal variability in cloud droplet number to reproduce the radiative effects of complex models.

- The simulated moisture flux into extratropical cyclone clouds is sensitive to resolution and very high-resolution models match observations well. In addition, complex cloud microphysics are required to have confidence in the cloud response to aerosol changes and climate change. Cloud radiative effects are not sensitive to resolution on a global average but higher resolutions lead to regional improvements. In contrast, cloud radiative effects are very sensitive to model complexity, initial conditions of the simulations, and the coupling between atmosphere and ocean.

- The transition between stratocumulus and cumulus cloud regimes is an important aspect of global cloud climatology that is challenging for climate models to reproduce with fidelity. Focusing on the Atlantic transition, which is more relevant to European climate, suggests that the large-scale climatology is not sensitive to resolution and complexity. However, from a more quantitative perspective, cloud water content and rain rates depend on resolution and simple prescriptions of aerosol-cloud interactions produce thicker clouds and lower rain rates.

These conclusions are reassuring for model developments based on simplified representations of aerosols. There are notes of caution, however. First, it is not known whether biases remain consistent with pre-industrial and present-day conditions when simulating future scenarios. Second, even if radiative fluxes remain robust, the existence of changes in cloud water content may lead to differences in future climate feedbacks.

There have been no sizeable deviations from the proposed work.

2. Project Objectives

With this deliverable, the project has contributed to the achievement of the following objectives (DOA, Part B Section 1.1) WP numbers are in brackets:

No.	Objective	Yes	No
A	To develop a new generation of global high-resolution climate models. *(3, 4, 6)*	X	
B	To develop new strategies and tools for evaluating global high-resolution climate models at a process level, and for quantifying the uncertainties in the predictions of regional climate. *(1, 2, 5, 9, 10)*	X	
C	To provide new high-resolution protocols and flagship simulations for the World Climate Research Programme (WCRP)'s Coupled Model Intercomparison Project (CMIP6) project, to inform the Intergovernmental Panel on Climate Change (IPCC) assessments and in support of emerging Climate Services. *(4, 6, 9)*		X
D	To explore the scientific and technological frontiers of capability in global climate modelling to provide guidance for the development of future generations of prediction systems, global climate and Earth System models (informing post-CMIP6 and beyond). *(3, 4)*	X	
E	To advance understanding of past and future, natural and anthropogenic, drivers of variability and changes in European climate, including high impact events, by exploiting new capabilities in high-resolution global climate modelling. *(1, 2, 5)*		X
F	To produce new, more robust and trustworthy projections of European climate for the next few decades based on improved global models and advances in process understanding. *(2, 3, 5, 6, 10)*		X
G	To engage with targeted end-user groups in key European economic sectors to strengthen their competitiveness, growth, resilience and ability by exploiting new scientific progress. *(10, 11)*		X
H	To establish cooperation between science and policy actions at European and international level, to support the development of effective climate change policies, optimize public decision making and increase capability to manage climate risks. *(5, 8, 10)*		X

3. Detailed Report

3.0 Introduction

Changes in aerosol concentrations and cloudiness exert a forcing of top-of-atmosphere and surface radiative fluxes, which in turn modifies surface temperature and the hydrological cycle. PRIMAVERA Stream 1 simulations used diverse horizontal resolutions, so there is a need to explore the impact of resolution on simulated radiative fluxes, cloudiness, and precipitation. In addition, aerosol concentrations are prescribed in a consistent way in all core simulations (see WP6 deliverables), thus partly suppressing the long-standing inter-model diversity in aerosol and cloud radiative forcing, trends, and climate response, but with a loss of correlation between aerosols and clouds that could affect aerosol radiative forcing and climate response. There is therefore a need to quantify the need for improved representation of clouds and aerosols in a high-resolution environment.

This deliverable describes the results obtained by PRIMAVERA activities in WP3a. The aim was to compare different simulations covering different corners of the complexity/resolution space (Figure 0.1), focusing on simulated radiative fluxes, clouds, and aerosol-cloud interactions.

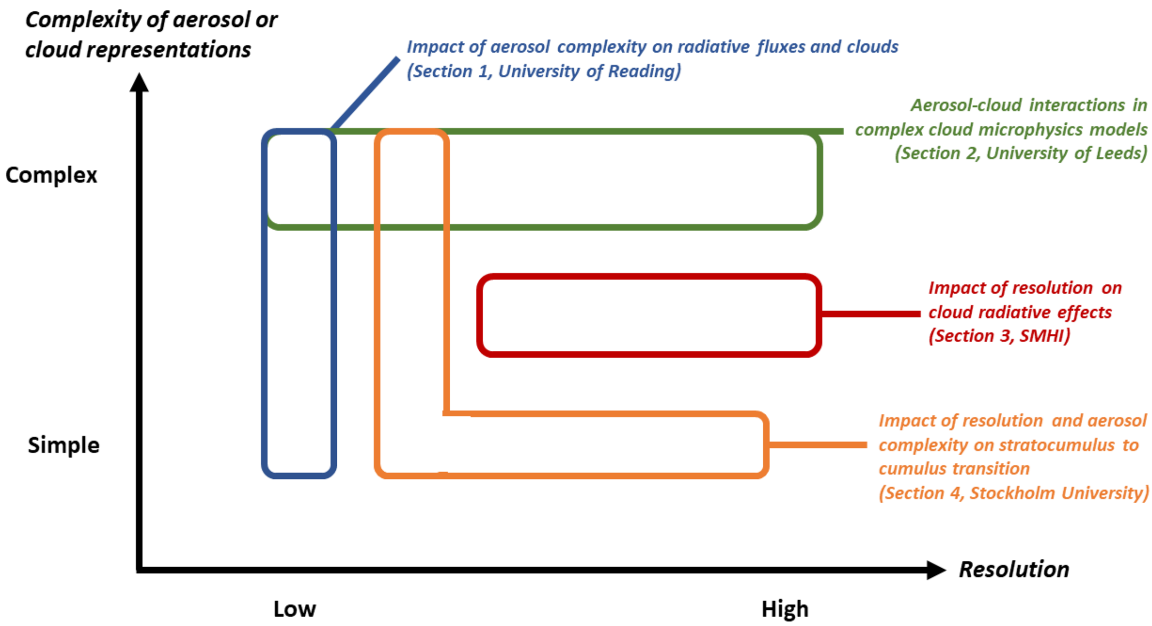

Figure 0.1: *Schematic summary of the work described in this deliverable, and how it samples different corners of the complexity (y-axis) / resolution (x-axis) space.*

More specifically, in this deliverable the PRIMAVERA Stream 1 ensemble and additional simulations were exploited to:

- Assess whether prescribed (rather than interactive) aerosols produce realistic radiative forcing and responses despite a lack of consistency with the modelled clouds and precipitation (sections 1 and 4);

- Compare core simulations to additional simulations of aerosol-radiation-cloud interactions at convection-permitting scales to identify potential biases introduced by lower resolution dynamics and microphysics complexity (section 2);
- Quantify the robustness of the simulated energy budget, clouds, and precipitation across models and resolutions (sections 3 and 4).

3.1 Impact of aerosol complexity on radiative fluxes and clouds

Gill Thornhill and Nicolas Bellouin (University of Reading)

In this section, we examine how the complexity of the representation of aerosols in a climate model influences modelled radiative fluxes and the characteristics of modelled clouds. The model used here is the atmosphere-only GA7.1 configuration of Hadley Centre Global Environmental Model version 3 (HadGEM3) (Walters et al., 2017). That model uses the Global Model of Aerosol Processes (GLOMAP) (Mann et al., 2010), the Prognostic Cloud fraction Prognostic Condensate (PC2) cloud scheme (Wilson et al., 2008), and the Suite Of Community RAdiative Transfer (SOCRATES) (a rewritten version of Edwards and Slingo 1996) radiative transfer code. GLOMAP simulates aerosol mass and number concentrations in five size modes, and represents primary emission, nucleation of new particles, condensation from the gas phase, coagulation, ageing, and dry and wet deposition, so is numerically expensive to run. Consequently, HadGEM3 uses for in PRIMAVERA Stream 1 simulations a simplified, prescribed set of aerosol optical properties and cloud droplet number concentrations (CDNC) to reduce computational cost. There is therefore a need to check that using prescribed aerosols reproduces the aerosol radiative effect and forcing, and cloud fraction and water content, simulated by the more complex model.

We have run pairs of 20-year simulations (Table 1.1). The first simulation uses the standard HadGEM3 GA7.1 configuration, with aerosols modelled by GLOMAP. Dedicated diagnostics provide aerosol extinction, absorption, and asymmetry parameter averaged over the 6 shortwave and 9 longwave wavebands used by the SOCRATES radiative transfer code of HadGEM3, and CDNC. Those diagnostics are then averaged monthly and used as inputs to an aerosol prescription system called EasyAerosol (Stevens et al. 2017). CDNC includes the impact of aerosol changes and is used in the calculation of liquid cloud albedo and auto-conversion rate from liquid cloud water to rain water, which affects precipitation rates. There are no interactions between aerosols and ice clouds in HadGEM3. The only difference between the two simulations is the way aerosols are represented: GLOMAP and EasyAerosol-from-GLOMAP. Two pairs of GLOMAP simulations where runs, using emissions representative of pre-industrial (1850) and present-day (2014) conditions, respectively. In the following, we present differences between each pair, averaged over the 20 years of simulations. Looking at shorter periods within those 20 years and seasonally does not change the conclusions.

Simulation name	Aerosol scheme	Emissions / Prescriptions
GLOMAP_PI	GLOMAP	Emissions for 1850
EASY_PI	EasyAerosol	Prescription from GLOMAP_PI
GLOMAP_PD	GLOMAP	Emissions for 2014
EASY_PD	EasyAerosol	Prescriptions from GLOMAP_PD

Table 1.1 *List of HadGEM3 simulations used in Section 1.*

Figure 1.1 shows differences in globally- and 20-year averaged radiative fluxes and effective radiative forcing, which is computed as the difference between radiative fluxes in present-day and pre-industrial simulations. All differences are statistically significant at the 95% confidence level. All-sky differences remain significant at the 99% confidence level, but clear-sky differences become insignificant. The largest differences are seen in the all-sky shortwave radiative flux, with large differences also seen in all-sky longwave component. Differences in clear-sky (cloud-free) radiative fluxes are small, suggesting that differences in all-sky radiative fluxes are due to changes in the radiative properties of clouds. Differences in effective radiative forcing are small compared to differences in absolute radiative fluxes, suggesting that systematic biases introduced by the EasyAerosol prescription partially cancel out when subtracting present-day from pre-industrial distributions.

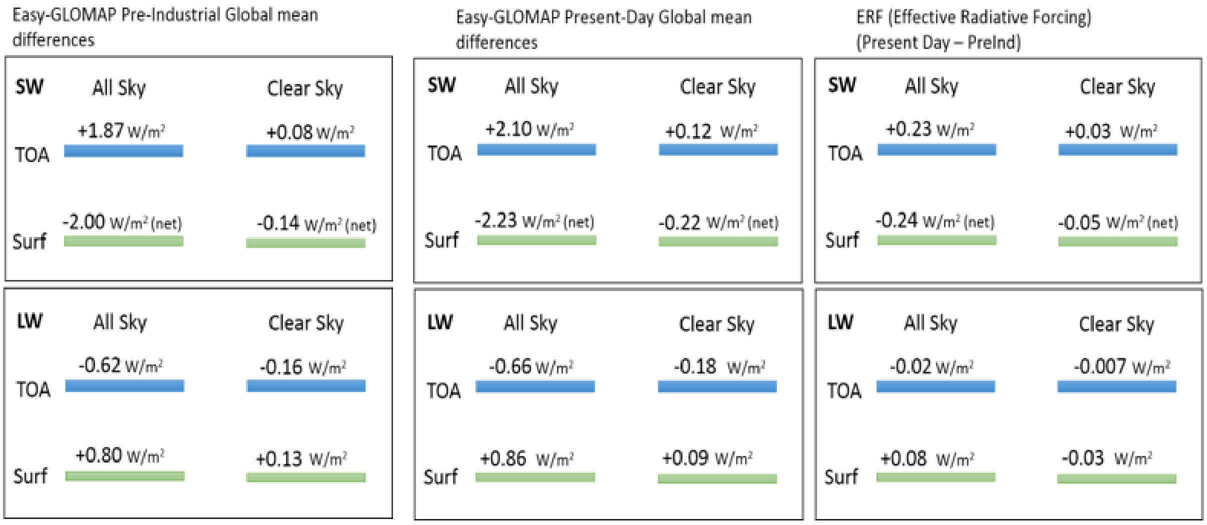

Figure 1.1: *Differences in globally- and 20-year averaged radiative fluxes, in W m^{-2}, between EasyAerosol and GLOMAP simulations for pre-industrial (left column) and present-day aerosols (middle column). The right column shows differences in EasyAerosol and GLOMAP effective radiative forcing between present-day and pre-industrial simulations. TOA and Surf stand for Top Of Atmosphere and Surface, respectively.*

Figure 1.2 shows the distributions of differences in top-of-atmosphere outgoing shortwave radiative flux and cloud fraction. EasyAerosol reflects an excess of 2.1 W m^{-2} compared to GLOMAP, with the differences being statistically significant across a large proportion of the globe. Radiative flux differences are well correlated with changes in cloud fraction, suggesting those changes are at least partly responsible for the discrepancies in radiative fluxes.

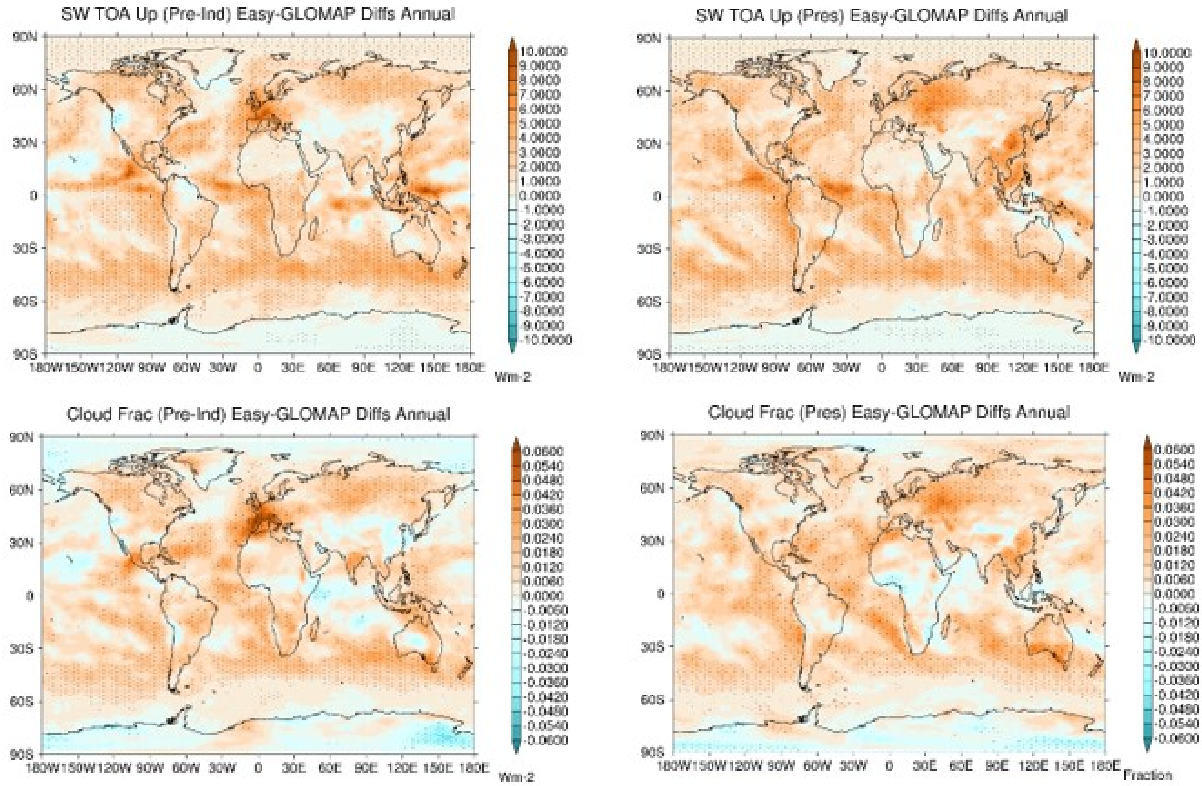

Figure 1.2: *Differences between simulations using EasyAerosol and GLOMAP for shortwave top-of-atmosphere (TOA) outgoing flux (top row, in W m^{-2}) and cloud fraction (bottom row). Left column is for pre-industrial conditions, right column is for present-day conditions. Stippling indicates statistically significant differences at the 95% confidence level.*

Differences could also be ascribed to changes in cloud thickness. Figure 1.3 shows simulated liquid, ice, and vapour water content. Liquid Water Path (LWP) increases in the EasyAerosol simulation and exhibits differences that correlate with differences in cloud fraction to a large extent. Ice Water Path (IWP) changes are much less statistically significant than LWP, as expected in a model where aerosols do not interact with ice clouds. Precipitable Water Content (PWC) shows some significant differences, most clearly seen to the west of South America and Africa in both the pre-industrial and present-day cases. That may indicate a relationship with the stratocumulus cloud regime or shallow convection in general. Pre-industrial differences in LWP are particularly large in Europe, while present-day differences are more diffuse and present a local peak over Asia. Such patterns suggest that differences are co-located with the largest aerosol concentrations. Cloud droplet effective radius is reduced in the EasyAerosol simulation compared to the GLOMAP simulation, especially at lower altitudes.

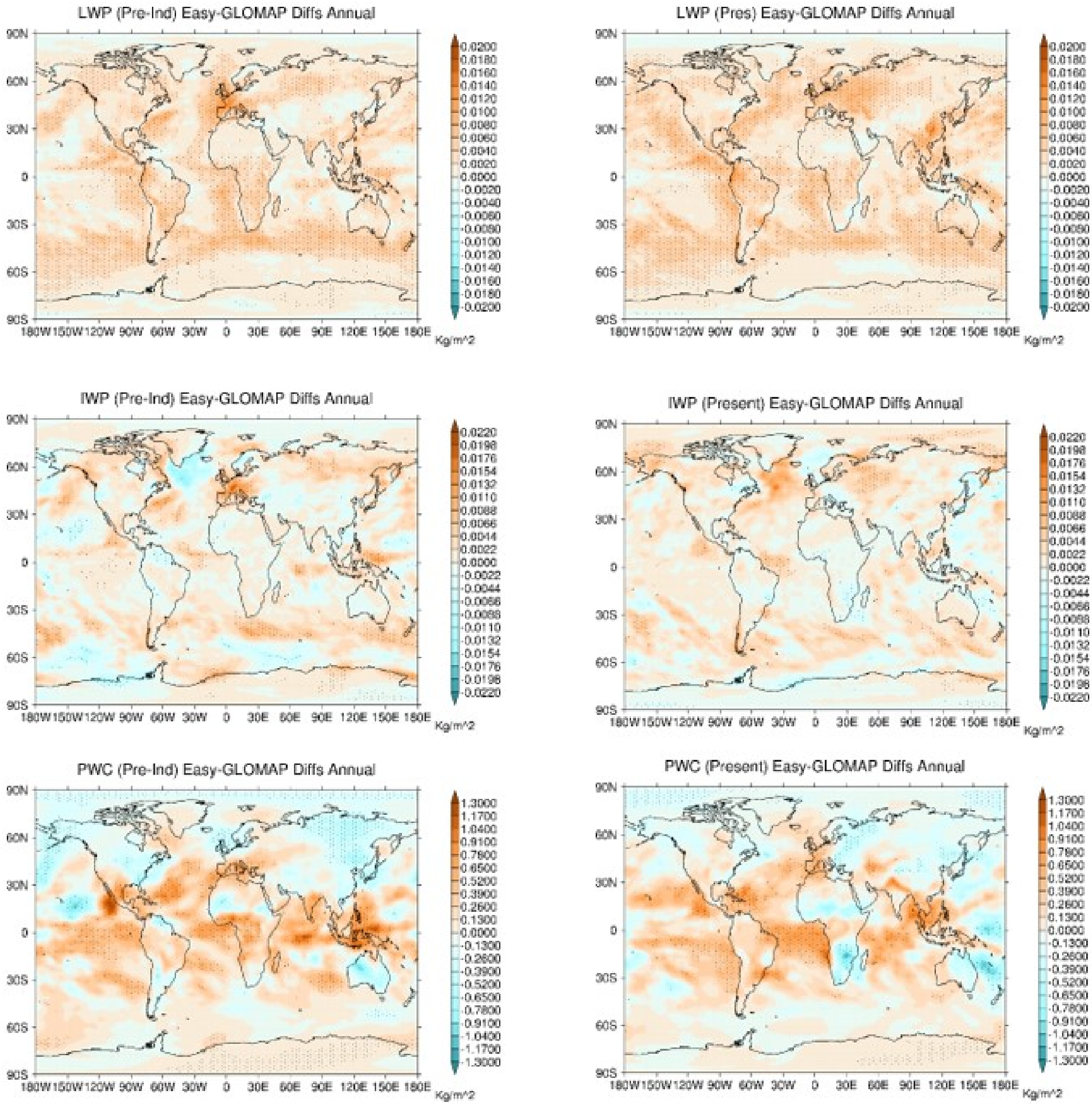

Figure 1.3: *Differences in (from top to bottom) liquid water path, ice water path and precipitable water content (all in kg m*$^{-2}$*) between the EasyAerosol simulations and the GLOMAP simulations. Left column is for pre-industrial conditions, right column is for present-day conditions. Stippling indicates statistically significant differences at the 95% confidence level.*

To better understand the role of atmospheric water in differences in liquid water content, we examined globally-averaged evaporation, precipitation and residence time of water in the atmosphere over the 20 simulated years (Table 1.2). As expected from a balanced water budget, globally-averaged evaporation closely matches globally-averaged precipitation in all simulations. There is more water available in the atmosphere in the EasyAerosol simulation and the residence time of water in the atmosphere is longer. This indicates that more atmospheric water is available in the EasyAerosol simulation to form more, thicker clouds. The increase in evaporation can be traced back to an increase in surface latent heat flux, but it is difficult to separate the driver of that increase from the response to increased cloudiness.

Water flux ($kg\ m^{-2}$)	Pre-industrial		Present-day	
	GLOMAP	EasyAerosol	GLOMAP	EasyAerosol
Evaporation	1132.71	1135.83	1130.12	1132.69
Atmospheric water	23.55	23.67	23.55	23.64
Precipitation	1133.05	1136.25	1130.46	1133.13
Residence Time (days)	7.57	7.61	7.59	7.62

Table 1.2: *Characteristics of the atmospheric water cycle in HadGEM3 simulations with GLOMAP and EasyAerosol, in pre-industrial and present-day conditions.*

The relationship between CDNC and cloud albedo is non-linear (Taylor and McHaffie, 1994). Consequently, prescribing mean CDNC does not translate into mean cloud albedo. Modellers working on the Community Atmosphere Model found discrepancies like those described above when using a monthly prescribed aerosol scheme. To ensure that the CDNC space and the associated non-linearities are properly sampled, they introduced random temporal variability by prescribing the mean and standard deviation of the CDNC distribution, assumed to be lognormal. Following their results, we ran a one-year present-day simulation with GLOMAP to obtain monthly-averaged CDNC variance over 3-hourly intervals, 3 hours being the HadGEM3 radiation code time step. A new simulation, EASY_PDvar was configured to repeat the EASY_PD simulation, but now prescribing both monthly-averaged CDNC and its variance, and randomly selecting a CDNC value within the lognormal distribution defined by those two parameters. Results show that accounting for temporal variability reduces the all-sky discrepancy in the EasyAerosol simulation substantially (Table 1.3). Differences in all-sky outgoing shortwave radiative flux are reduced by 0.8 W m^{-2} (38%) to +1.3 W m^{-2}. Differences in cloud fraction are also reduced and get closer to interannual variability.

	GLOMAP_PD	Easy_PD	Easy_PDvar	Easy_PD minus GLOMAP_PD	EasyPDvar minus GLOMAP_PD
Outgoing shortwave flux at TOA ($W\ m^{-2}$)	100.35 ± 0.13	102.45 ± 0.12	101.61 ± 0.18	+2.10 ± 0.14	+1.26 ± 0.20
Net shortwave flux at surface ($W\ m^{-2}$)	166.73 ± 0.15	164.50 ± 0.16	165.40 ± 0.23	−2.23 ± 0.18	−1.33 ± 0.23
Cloud fraction	0.690 ± 0.002	0.699 ± 0.003	0.695 ± 0.002	+0.009 ± 0.003	+0.005 ± 0.003

Table 1.3: *Globally-averaged radiative fluxes and cloud fraction in present-day simulations using GLOMAP, EasyAerosol, and EasyAerosol with account for cloud droplet number variance, and their differences.*

Figure 1.4 shows the distributions of differences in top-of-atmosphere outgoing shortwave radiative flux and cloud fraction in the EASY_PDvar simulation. Accounting for CDNC variability greatly reduces the areas of significant differences with GLOMAP for both variables. However, cloud fraction remains larger in the EasyAerosol simulation, especially over stratocumulus decks. Nevertheless, the improvement from the original EasyAerosol comparisons is substantial. Differences in LWP, IWP and PWC are also reduced (not shown).

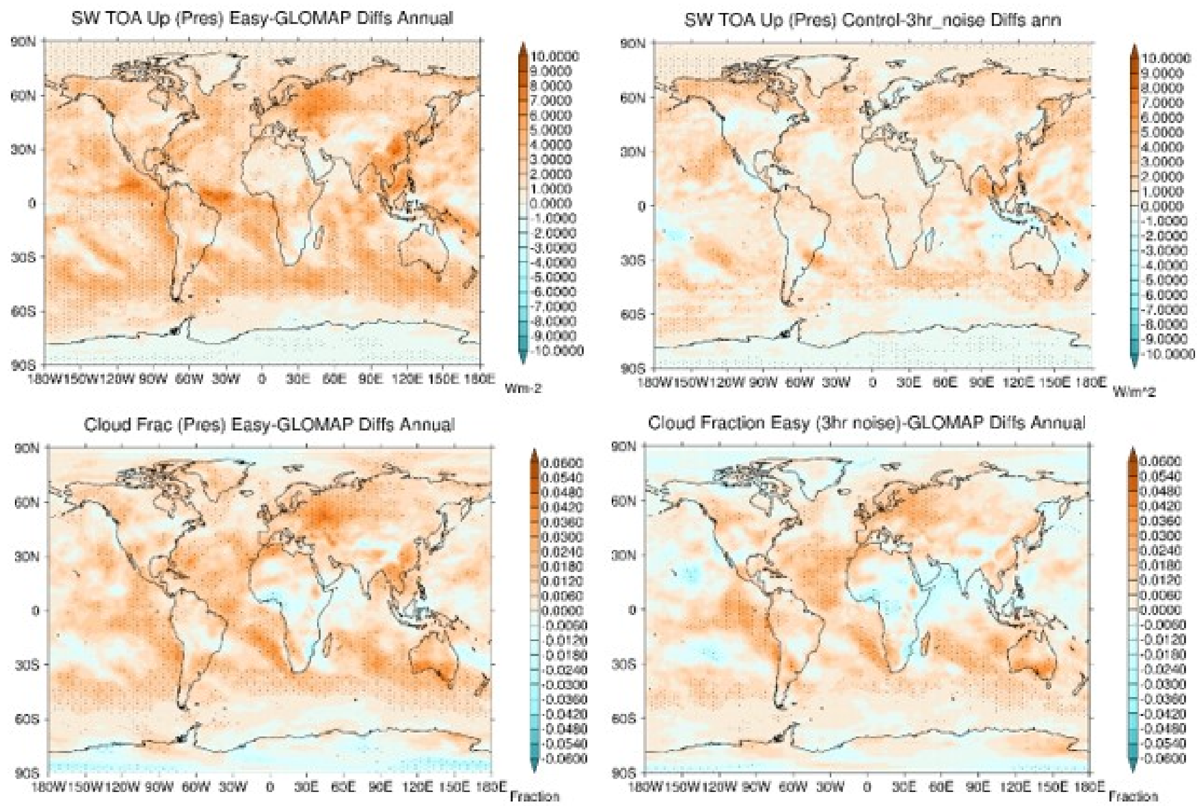

Figure 1.4: *Differences between present-day simulations using EasyAerosol and GLOMAP for shortwave top-of-atmosphere (TOA) outgoing flux (top row, in W m^{-2}) and cloud fraction (bottom row). The left column shows differences when only mean cloud droplet number concentrations are prescribed. Stippling indicates statistically significant differences at the 95% confidence level.*

Figure 1.5 summarises the results discussed in this section. The use of EasyAerosol to provide a more computing-efficient alternative to a fully interactive aerosol scheme such as GLOMAP preserves clear-sky (cloud-free) fluxes but introduces relatively large differences in all-sky fluxes. Those differences were traced back to having more, thicker clouds in the EasyAerosol simulation, caused by a longer residence time of water in the atmosphere. It is hypothesised that the issue revolves around non-linearities in the CDNC-albedo and CDNC-auto-conversion relationships, which imply that mean CDNC does not yield mean cloud albedo and auto-conversion rates. Accounting for temporal variability in CDNC over the 3-hour radiation code time step reduces differences significantly.

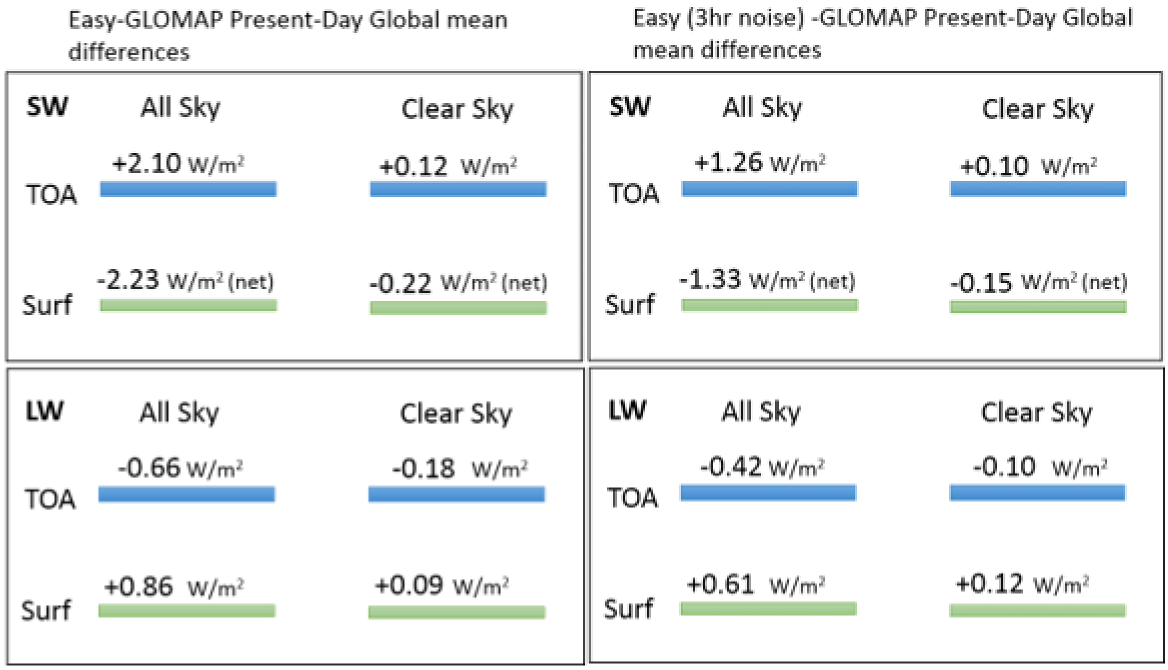

Figure 1.5: *Differences in globally- and 20-year averaged radiative fluxes, in W m^{-2}, between EasyAerosol and GLOMAP simulations for present-day aerosols. The left column shows differences when only mean cloud droplet number concentrations are prescribed. The right column shows differences when also prescribing cloud droplet number variance. TOA and Surf stand for Top Of Atmosphere and Surface, respectively.*

Key points:

- Prescribing aerosol optical properties maintains radiative balance in clear-sky, but prescribing cloud condensation nuclei causes a large imbalance in all-sky conditions. This imbalance does not fully propagate to the effective radiative forcing, however, because similar biases in present-day and pre-industrial conditions cancel out.
- Differences in all-sky radiative fluxes are traced back to the prescription of cloud droplet number concentrations creating more, thicker clouds because of a slower hydrologic cycle.
- Non-linearities in cloud physics mean that prescribing mean cloud droplet number concentrations does not yield mean cloud properties. Accounting for variance in cloud droplet number concentrations strongly reduces the differences caused by the prescriptions.

3.2 Aerosol-cloud interactions in complex cloud microphysics models

Daniel McCoy and Paul Field (University of Leeds)

This section examines the effects of aerosol on the clouds in midlatitude cyclones and how model resolution affects the prediction of lightning. To constrain aerosol-cloud interactions we have harnessed very high resolution (~7 km horizontal grid spacing) simulations in the UK MetOffice Unified Model (UM) using the new CASIM cloud microphysics scheme (UM-CASIM) (Hill et al., 2015). By doing this we have been able to show that cloud adjustments within midlatitude weather systems lead to a negative radiative forcing (which is a subject of considerable debate (Malavelle et al. 2017; Sato et al. 2018). In the process of pursuing this investigation we leveraged our improved knowledge of aerosol-radiation-cloud interactions to better understand the response of extratropical cyclones to warming. We were able to combine the results of our very high-resolution UM simulations with other PRIMAVERA models and other institutes' high-resolution simulations (ICON (Giorgetta et al. 2018), NICAM (Kodama et al. 2015)) to propose a new set of cloud feedbacks within the midlatitudes. Finally, high-resolution simulations within the UM were used to show that observed patterns of lightning can be reproduced within a global model. We will describe each of these investigations in more detail below.

As noted above, the adjustment of clouds to aerosol is a poorly constrained aspect of aerosol-cloud interactions. Here, we examine the response of midlatitude cyclone cloud properties to a change in cloud droplet number concentration (CDNC). Idealized experiments in high-resolution, convection-permitting global aquaplanet simulations with constant CDNC are compared to thirteen years of remote-sensing observations. Observations and idealized aquaplanet simulations agree that increased warm conveyor belt (WCB) moisture flux into cyclones is consistent with higher cyclone liquid water path (CLWP) as shown in Figure 2.1. When CDNC is increased a larger LWP is needed to give the same rain rate. The LWP adjusts to allow the rain rate to be equal to the moisture flux into the cyclone along the warm conveyor belt. This results in an increased CLWP for higher CDNC at a fixed WCB moisture flux in both observations and simulations. If observed cyclones in the top and bottom tercile of CDNC are contrasted it is found that they not only have higher CLWP, but also cloud cover, and albedo. The difference in cyclone albedo between the cyclones in the top and bottom third of CDNC is observed by CERES to be between 0.018 and 0.032, which is consistent with a 4.6-8.3 Wm^{-2} in-cyclone enhancement in upwelling shortwave when scaled by annual-mean insolation. Based on a regression model to observed cyclone properties, roughly 60% of the observed variability in CLWP can be explained by CDNC and WCB moisture flux. The recent fissure eruption at Holuhraun was examined within this framework and confirmed that, given the meteorology during that period, the cyclone clouds in that region had a higher CLWP (McCoy et al. 2018).

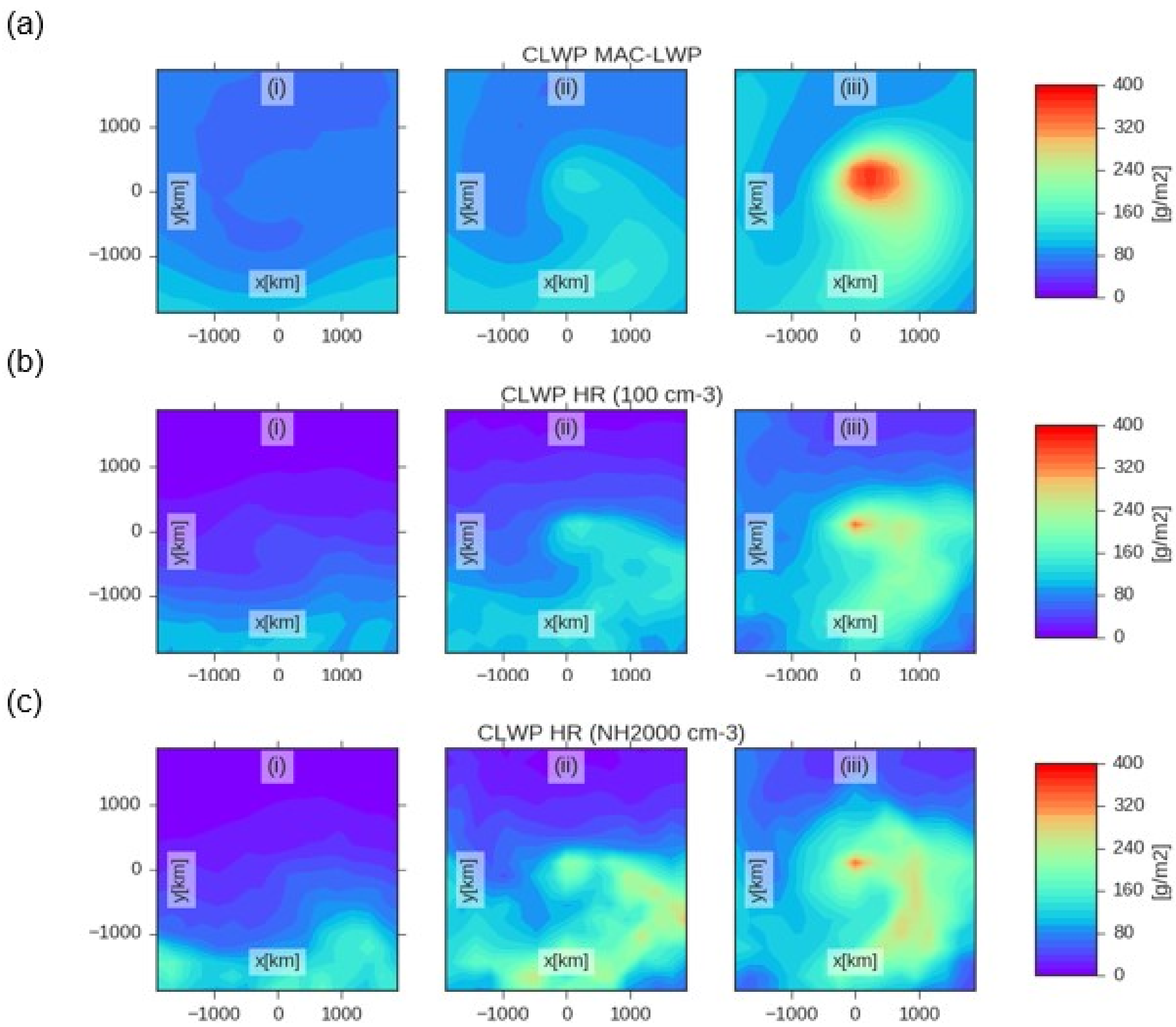

Figure 2.1: *Cyclone liquid water path (CLWP, rain and cloud water, in g m^{-2}) composited around cyclone centers in (a) the observations from the Multi-sensor Advanced Climatology of LWP (Elsaesser et al. 2017), (b) the UM-CASIM simulations at low CDNC, and (c) the UM-CASIM simulations at a high CDNC.*

As we described above, using idealized simulations we were able to propose a new framework for understanding variability in clouds within extratropical cyclones. This framework was set within the context of aerosol-cloud interactions. However, this framework also allowed us to gain insight into the way that these clouds change in response to global warming. The change in shortwave cloud radiative forcing in response to warming is the leading uncertainty term in model-predicted climate sensitivity (Caldwell et al. 2016). We can gain insight into the shortwave cloud feedback from examining cyclone variability. We contrasted global climate models (GCMs) with horizontal resolutions from 7 km (the UM-CASIM simulations described above), through the tiered resolutions of the PRIMAVERA simulations, up to horizontal resolutions of hundreds of kilometres (traditional GCMs from CMIP5) with Multi-Sensor Advanced Climatology Liquid Water Path (MAC-LWP) microwave observations of cyclone properties from the period 1992-2015. As we found in our previous work looking at aerosol-cloud interactions, inter-cyclone variability in both observations and models is strongly driven by moisture flux along the cyclone's WCB. Stronger WCB moisture flux enhances liquid water path (LWP) within cyclones. This relationship is replicated in

GCMs, although its strength varies substantially across models (Figure 2.2). In the southern hemisphere (SH) oceans 28-42% of the observed interannual variability in cyclone LWP may be explained by WCB moisture flux variability. This relationship was used to propose two cloud feedbacks acting within extratropical cyclones: a negative feedback driven by Clausius-Clapeyron increasing water vapor path (WVP), which enhances the amount of water vapor available to be fluxed into the cyclone; and a feedback moderated by changes in the life cycle and vorticity of cyclones under warming, which changes the rate at which existing moisture is imported into the cyclone. We show that changes in moisture flux drive can explain the observed trend in Southern Ocean cyclone LWP (Manaster et al. 2017) over the last two decades. Transient warming simulations show that the majority of the change in cyclone LWP can be explained by changes in WCB moisture flux, as opposed to changes in cloud phase (McCoy et al. 2015). The variability within cyclone composites was examined to understand what cyclonic regimes the mixed phase cloud feedback is relevant to. At a fixed WCB moisture flux cyclone LWP increases with increasing SST in the half of the composite poleward of the low and decreases in the half equatorward of the low in both GCMs and observations. Cloud-top phase partitioning observed by the Atmospheric Infrared Sounder (AIRS) indicated that phase transitions may be driving increases in LWP in the poleward half of cyclones (McCoy et al. 2018).

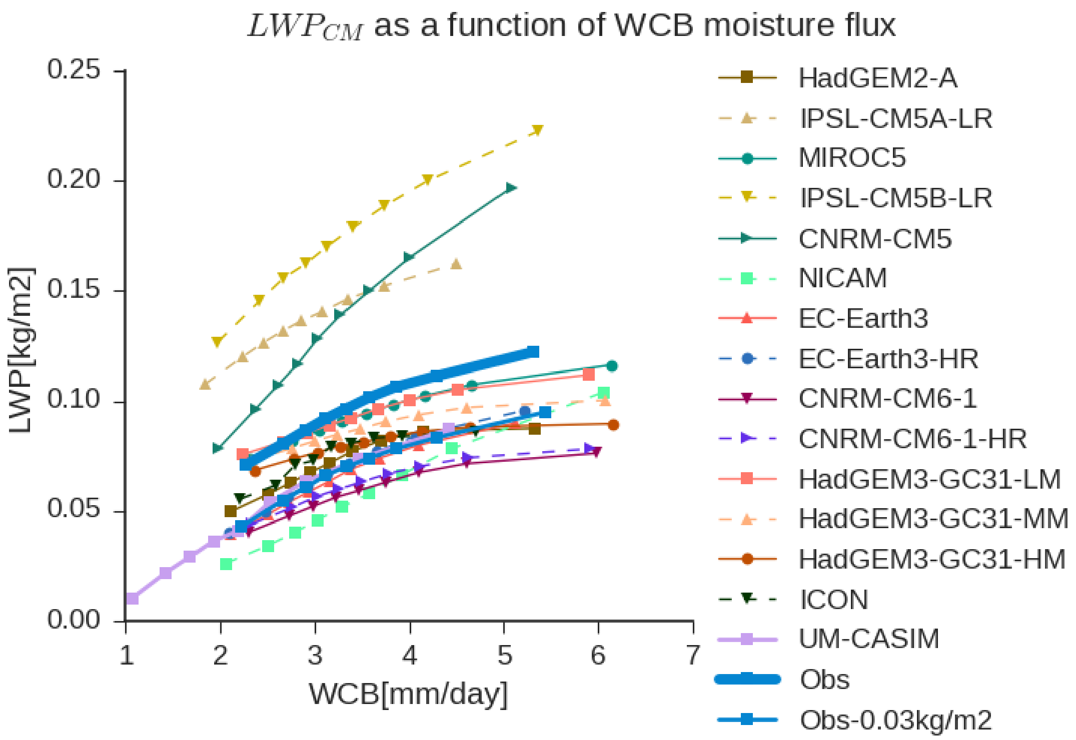

Figure 2.2: *Liquid Water Path (only within clouds, not including rain) composited around cyclone centres as a function of WCB moisture flux as observed by MAC-LWP and simulated by an array of models. Models shown here are the UM-CASIM 7 km simulations, PRIMAVERA historical simulations, CMIP5 CFMIP2 simulations, NICAM, and ICON.*

High resolution (grid spacing ~10 km in midlatitudes) model simulations using explicitly resolved convection in the Met Office Unified Model were used to provide a global lightning climatology. The results show for the first time that global simulations can capture the strong diurnal flash rate variation as well as the seasonal variation. Comparisons were made with the World Lightning Location Network and combined LIS, OTD dataset. The model results generally capture the temporal behaviour and spatial distribution of the lightning over land. Over the ocean the lightning in the ITCZ appears excessive (Field et al. 2018). Low-resolution models simulate a diurnal peak in convection around local noon, whereas lightning over major continental regions is observed to peak in the afternoon.

Key points:

- Very high-resolution global models and observations agree that the moisture flux into extratropical cyclones is a key factor in determining the amount of cloud within the cyclone. Moisture flux into cyclones will increase as the climate warms, leading to a negative shortwave cloud feedback.
- Using the moisture flux, we can remove enough meteorological variability from extratropical cyclone clouds to see a signal from aerosol-cloud adjustments, confirming that the aerosol radiative forcing from clouds within midlatitude low pressure systems is negative.
- High resolution global models have the capability to reproduce the observed climatology of lightning, while low-resolution models fail to reproduce the diurnal cycle correctly.

3.3 Impact of resolution on cloud radiative effects

Manu Anna Thomas, Torben Koenigk, and Klaus Wyser (SMHI)

In this section, the surface (SFC) and top of the atmosphere (TOA) cloud radiative effects (CREs) in 4 global climate models (Table 3.1) with varying resolutions adding up to a total 9 different set-ups were evaluated using satellite observations from the NASA's CERES-EBAF (Clouds and the Earth's Radiant Energy System-Energy Balanced And Filled) instrument. Apart from this, the cloud radiative response to two leading modes of natural variabilities, namely ENSO and NAO, is evaluated allowing process-oriented studies. The simulations from the high (Hi-res) and low-resolution model set-ups (Std-res) were contrasted to investigate if any value can be added by increasing the spatial resolution of the different models.

Models used	**Grid resolution**	**Atmosphere**
HadGEM3-GC31-HM	N512L85	MetUM-GA7.1
HadGEM3-GC31-MM	N216L85	MetUM-GA7.1
HadGEM3-GC31-LM	N96L85	MetUM-GA7.1
EC-Earth3-HR	T511L91	IFS CY36r4
EC-Earth3	T255L91	IFS CY36r4
MPIESM-XR	T255L95	ECHAM6.3
MPIESM-HR	T127L95	ECHAM6.3
ECMWF-HR	Tco399L91	IFS CY43r1
ECMWF-LR	Tco199L91	IFS CY43r1

Table 3.1: *List of models analysed in this study. The models included in the Hi-res ensemble mean are HadGEM3-GC31-HM, EC-Earth3-HR, MPIESM-XR and ECMWF-HR. Their low-resolution counterparts are included in the Std-res ensemble mean.*

The largest disagreements in the SW CREs between models and observations occur over the polar regions, both at the TOA and the SFC in the summer hemisphere, and especially over the locations where seasonal sea-ice variability is strongest (Figure 3.1). In SH summer (DJF mean), all the models overestimate this forcing by up to 45 W m^{-2} over the coastal Antarctic and with the exception of the MPIESM models, the SW CREs do not respond to varying resolution in this region. The Std-res set up of the MPIESM model better simulates this response at the TOA and SFC than the Hi-res set up. However, in NH summer, the HadGEM3 model set ups overestimate the SW CREs over the Arctic by 10-15 W m^{-2}, whereas, all other models simulate a negative bias of magnitude 20—30 W m^{-2}. The surface SW CREs plays an important role during the melt season. These high discrepancies will have an implication for quantifying the cloud feedbacks on the sea-ice and estimating future changes in sea-ice during the melt season. The bias in SW and LW forcing in both the seasonal means over the tropics (30S-30N) at the TOA are of opposite sign, thereby nearly compensating the fluxes in this region. The biases in the LW CREs are also high in the polar regions at the SFC, most likely originating from the biases in describing dominant atmospheric processes such as the strength of temperature inversions and heat and moisture transport (Medeiros et al., 2011; Woods et al., 2017).

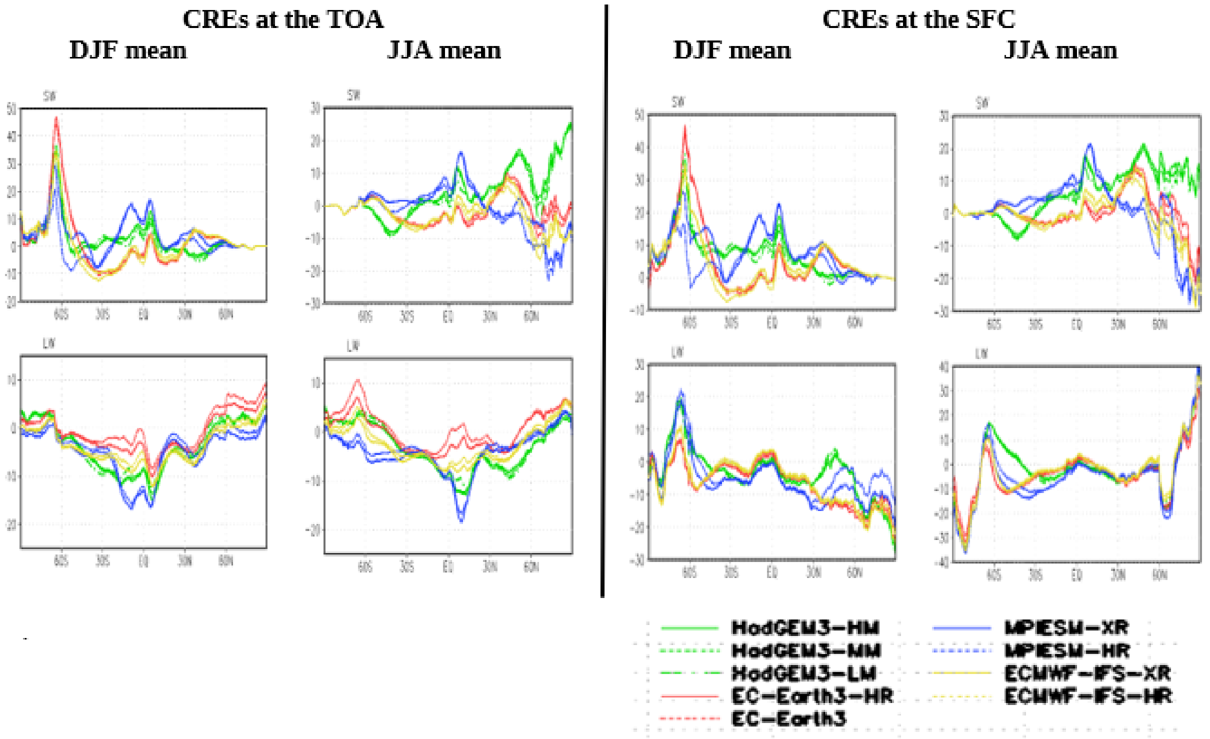

Figure 3.1: *Model simulated shortwave and longwave cloud radiative effects (CRE) in W m^{-2} shown as differences from observations at (left panels) the top-of-atmosphere (TOA) and (right panels) surface (SFC) for December-January-February (DJF) mean and June-July-August (JJA) mean.*

The zonally averaged cloud forcing does not seem to be resolution dependent. This means that all the models follow a similar response irrespective of the resolution at most regions. However, regional differences emerge when looking at the spatial patterns of the CRE differences between the Hi-res and Std-res set ups of the respective models. Here, it is seen that different cloud regimes are affected by increasing resolution in different models, where the HadGEM3 models show largest differences in the convective ITCZ regions, while MPIESM models over the Southern Oceanic stratocumulus region. In both these cases, the Hi-res set ups tend to overestimate the CREs in the SW at the TOA in DJF mean compared to their Std-res counterparts. Among the models. the most drastic change in resolution is occurring in the HadGEM3 models (from 200 km to 50 km). This may have impact on SST resampling and thus convection. In the case of Southern Oceanic clouds, the increasing resolution in MPIESM may change the humidity PDFs (probability distributions functions) in a way that would change cloud fraction (since the relative humidity is already persistently high in this region). And the lack of tuning in higher resolution versions can further explain the observed differences.

For the process-oriented evaluation, two major modes of natural variability, namely, ENSO and NAO, are chosen. All the models, irrespective of their resolutions simulate the spatial pattern of the cloud radiative response to ENSO and NAO reasonably well. However, stronger biases are observed in the magnitude of the signal. In general, the Std-res model set-ups simulate the response fairly well than their Hi-res model counterparts during ENSO events. The model biases are generally half as that of the actual cloud radiative response seen in the CERES data for the ENSO cases (5—10 W m^{-2}) at both TOA and the SFC, with

Hi-res model set ups simulating a stronger bias than the respective Std-res models. The biases in the LW forcing tend to be smaller than in the SW forcing. The inter-model differences in the SW forcing at the TOA and surface over the convectively active regions are stronger, nearly of the same order as the actual response. The inter-model differences in the LW forcing are lower at the surface during both ENP and ENN, typically within a few W m^{-2}. This suggests that the parameterization of SW radiative transfer and the treatment of cloud optical properties vary strongly among the models. The large-scale organization of convection and associated cloud types can also be different.

In the case of NAO, the model biases are less than observational uncertainties and well within the observational variability (less than one-sigma) in the cloud radiative anomalies. The spatial patterns of the response are also simulated quite well by the models during the positive and negative phases of the NAO. For example, the models, irrespective of their resolution, simulate the response reasonably well over the North Atlantic, Scandinavia and over the Mediterranean at the TOA in both SW and LW and at the SFC in SW. The models overestimate the cooling by 3-4 W m^{-2} over continental Europe in the SW at the TOA and SFC. The LW TOA CRE is, on the other hand, underestimated over this region. However, strong discrepancies can be noted in the SFC LW CREs with models overestimating the response by more than 5 W m^{-2} over northern Europe. Strong underestimation of similar magnitude in the LW CRE at the surface can be noted in the Canadian sector of the Arctic Ocean, and also over Greenland. The Hi-res model set-ups do not produce a significant improvement in the cloud radiative response owing to NAO events compared to their Std-res counterparts. The apparent insensitivity to increased resolution indicates that improving the surface parameterization schemes and their treatment (for example, snow and sea ice variability) is more important than only increasing the spatial resolution while simulating the CREs. These are atmospheric-only simulations and the response would be different or may be improved in coupled models where the SST (sea surface temperature) biases are smaller.

The analysis of the average absolute biases over the Niño3.4 region for the ENSO phases and over Europe (40W-40E, 30N-75N) for the NAO phases in the Hi-res and Std-res of each model shows that the absolute biases in both the cases are well below the uncertainty in the observational data. The average biases in the case of NAO are smaller than the biases seen over the Niño3.4 region. The Hi-res set up of HadGEM and EC-Earth models has a lower bias compared to their Std-res counterparts over the Niño3.4 region, whereas, an opposite signal is seen in MPIESM models. ECMWF model set ups exhibit the same biases irrespective of the resolution.

Key point:

- Increasing the spatial resolution do not automatically result in a substantial improvement in the cloud radiative effects, though some improvement is seen regionally. Other factors, such as fundamental parameterizations and process representation, surface descriptions, initial conditions, and atmosphere-ocean couplings, are likely to be more important.

3.4 Impact of spatial resolution and aerosol scheme complexity on simulations of stratocumulus to cumulus transition

Eva Nygren and Annica Ekman (Stockholm University)

In this section we investigate the influence of the horizontal model resolution and model aerosol complexity on the representation of stratocumulus to cumulus transition (SCT) in the Hadley Centre Global Environmental Model (HadGEM3) Global Coupled version 3.11 (HadGEM3-GC31, see also Section 3.1). The role of clouds in the Earth's climate system is one of the greatest challenges for studying both present climate and projections of the future. Representation of low marine stratocumulus is one particular weakness in General Circulation Models (GCMs). Improving our understanding and representation of marine stratocumulus and stratocumulus-to-cumulus transition, is a key task in model evaluation and diagnostics.

The analysis is based on model simulation outputs from PRIMAVERA Stream 1 where HadGEM3-GC31 was run in high (N512, 25 km), medium (N216, 60 km) and low (N96, 130 km) horizontal resolution with a non-interactive aerosol scheme (EasyAerosol), as well as a medium-resolution simulation run with a high complexity interactive aerosol scheme (GLOMAP). Table 4.1 summarises the simulations used. All four simulations were forced with prescribed SSTs for the years 1950-2014.

Simulation name	Resolution	Aerosol representation
HadGEM3-GC31-HM	N512	Non-interactive aerosols EasyAerosol
HadGEM3-GC31-MM	N216	Non-interactive aerosols EasyAerosol
HadGEM3-GC31-MM	N216	interactive aerosols GLOMAP
HadGEM3-GC31-LM	N96	Non-interactive aerosols EasyAerosol

Table 4.1: *List of simulations used in the analysis of section 4.*

The approach of studying cloud transition along a GCM transect approach was inspired by the GCSS/WGNE Pacific Cross-Section Intercomparison (GPCI) project (Teixeira et al., 2010) where a north east Pacific transect (GPCI transect) was defined as a simple framework for comparing SCT in weather prediction models and in GCMs. Here, the analysis focusses on a North East Atlantic (NEA) transect consisting of nine grid points which are similar for all different GCM grids (cf. description below). The transect stretches from the ocean region outside the North-western African continent and stretches south approximately aligned with the trade winds towards the equatorial region of the north eastern South American continent. The NEA transect captures the stratocumulus region in the North Eastern Atlantic basin, the deep convective region near the equator and the shallow cumulus region in between.

The grid positions of the NEA transect was determined based on Sandu et al. (2010) where air mass trajectories in the marine boundary layer transition regions were calculated using reanalysis data. A transect approximately parallel to the trajectory found in Sandu et al. (2010) was extracted from the HadGEM3 grid stretching from around 26°N and 26° W to around 9°N and 57° W, in latitudinal steps of around 2° and longitudinal steps of around 4°. Due to the different horizontal resolutions of the different model versions the grid point positions along the transect do not completely intersect and the closest grid points along the predefined transect were sampled in each simulation. Figure 4.1 shows the grid point position along the NEA transect in the different HadGEM3-CG31 resolution versions together with the trajectory calculated in Sandu et al. (2010). The one-year JJA climatology (2013) of sea surface temperature together with low cloud cover and high cloud cover based on reanalysis (ERA5) output is contoured in Figures 4.1a and 4.1b, respectively.

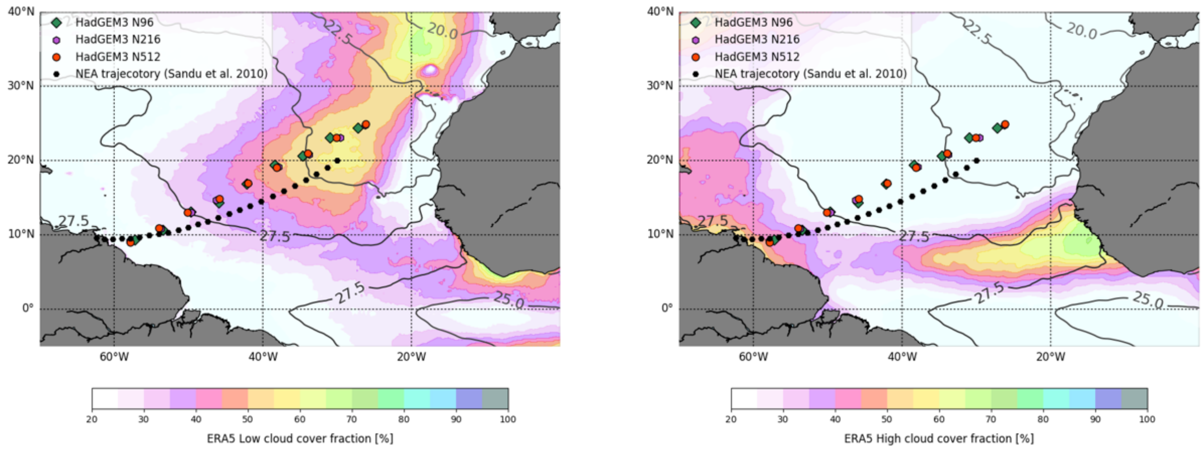

Figure 4.1: *Grid point positions along the North East Atlantic (NEA) transect for different horizontal resolution version of HadGEM3. Black dots mark the mean air mass trajectory from Sandu et al. (2010). Background map show the climatology of sea surface temperature (unfilled contours) and low cloud cover (left) and high cloud cover (right) for 2013 from ERA5 reanalysis.*

Figure 4.2 shows the mean vertical cross section of subsidence in Pa s^{-1} along the NEA transect in all versions of HadGEM3-CG31. The climatological mean is presented for the northern hemispheric summer season (JJA) and winter season (DJF). The NEA transect captures the subtropical-tropical part of the Hadley-circulation that we expect to find in this region, especially in the summer season. There is a dominating deep subsidence region in the south-western region and a shallow boundary layer in the north-eastern part of the transect. Only very small and non-significant differences in the mean wind speed and in the statistically-preferred wind direction along the transect are found between the different simulation versions and in the lower part of the atmosphere. Overall, the wind direction in and just above the model boundary layer is confirmed to be approximately aligned with the NEA transect, which is what we expect.

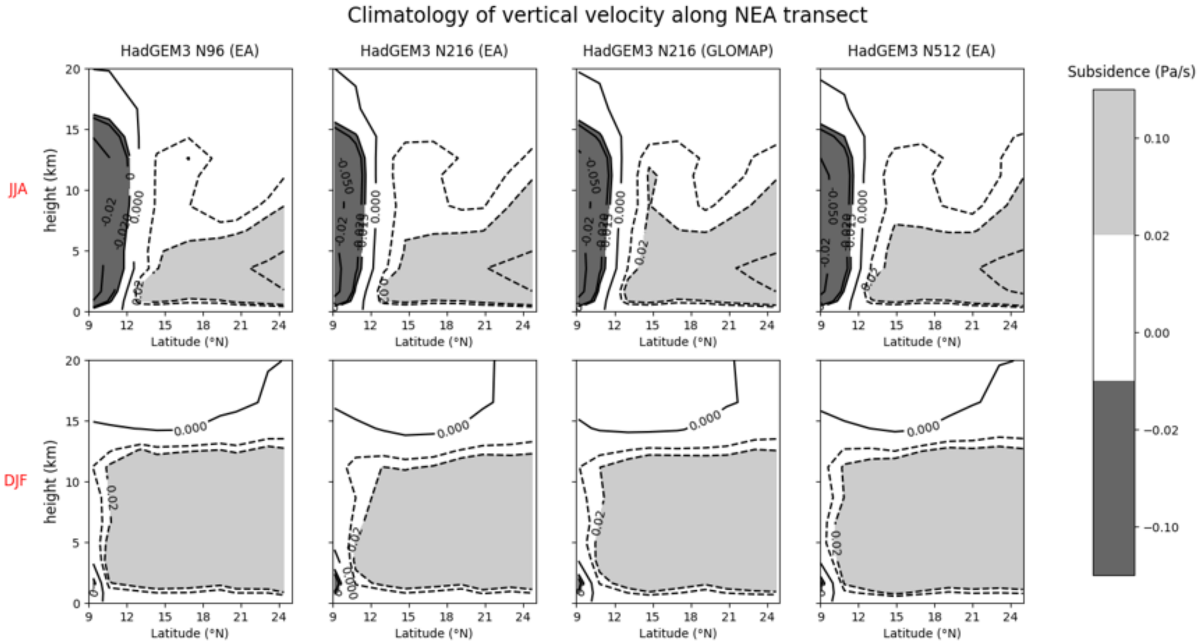

Figure 4.2: *Mean vertical cross section of subsidence (Pa s^{-1}) for all versions of HadGEM3-CG31 along the NEA transect. Upper panels show the north-hemisphere summer season (June-July-August) and lower panels show the winter season (December-January-February).*

Figure 4.3 shows the vertical cross section of cloud liquid water together with the mean cloud fraction for the JJA and DJF seasons. The vertical axis is logarithmic to accentuate the boundary layer cloud structure. It is again clear that we have sampled a transect in the HadGEM3-CG31 model that captures the SCT in the JJA season with the shallow and liquid boundary layer clouds in the north-eastern domain and the deep convective clouds in the southern parts. The figures show that neither the horizontal resolution nor the aerosol scheme complexity have a large impact on the representation of the clouds along the transect. There are some differences in mean cloud liquid water and cloud ice water between the N216 GLOMAP and EasyAerosol simulation, but the differences are in general very small and non-significant. The biggest (still small) differences between all simulations are found in the DJF season.

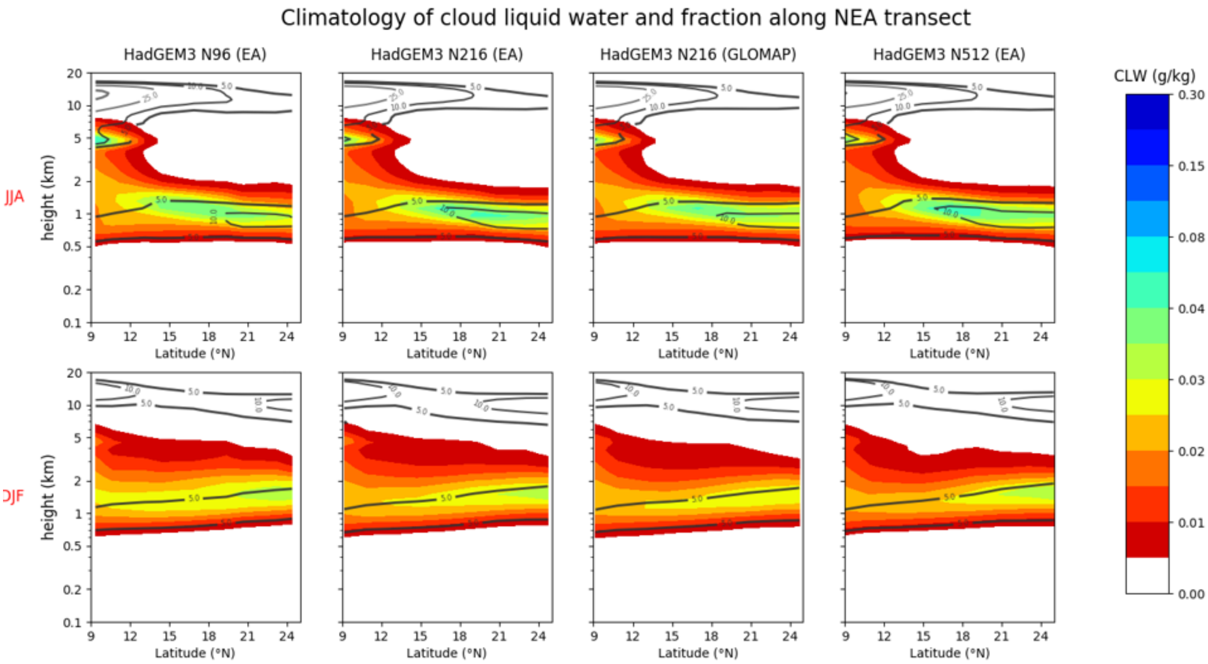

Figure 4.3: *Mean vertical cross section of cloud liquid water (filled contours) and cloud fraction (contours) along the NEA transect in different versions of HadGEM3-CG31. Upper panels show the north-hemisphere summer season (June-July-August) and lower panels show the winter season (December-January-February).*

Figure 4.4 shows the vertically-integrated cloud liquid water and cloud ice water for JJA and DJF for the different model versions. Dark blue circles mark where there is a significant difference between the N216 GLOMAP and EasyAerosol output. In the summer stratocumulus region (i.e. at the higher latitudes), differences in horizontal resolution and aerosol complexity generate very small differences in integrated liquid water. There is a small spread in the liquid and ice water path in the shallow cumulus and convective region where the low-resolution simulation has significantly higher water content that the high-resolution model. In the winter season, the spread between model versions is bigger. The N96 simulation has the highest mean cloud liquid water along the transect while N512 has the lowest, and the difference is significant. The difference between the GLOMAP and EasyAerosol mean is very small but significant at some positions along the transect. We do not find any significant difference in integrated ice water for the different simulations.

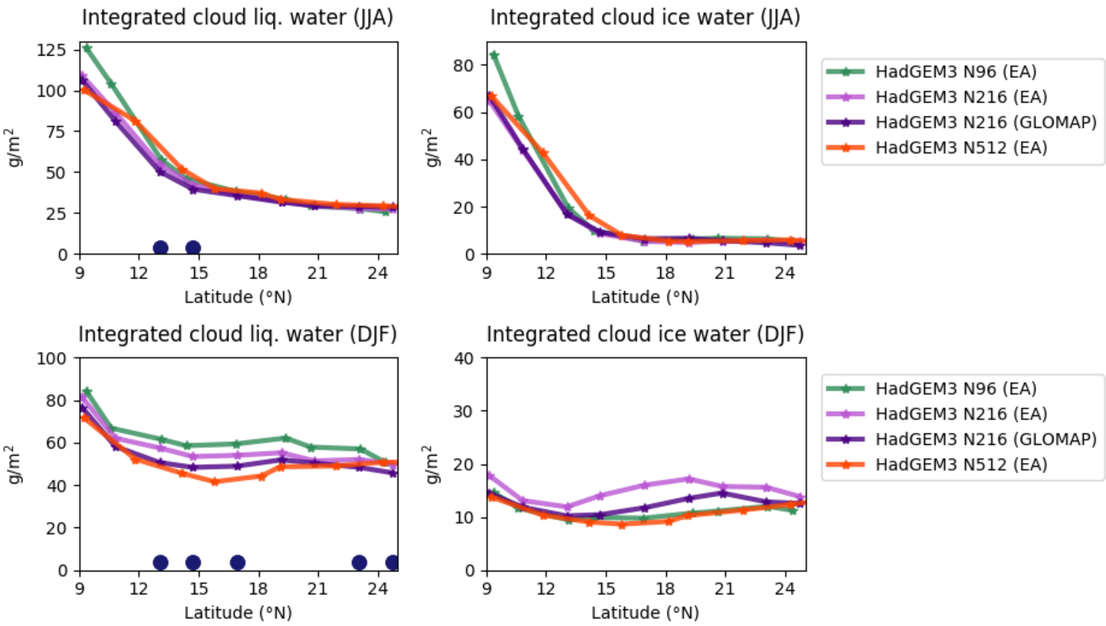

Figure 4.4: *Transect mean of integrated cloud liquid water (left) and integrated cloud ice water (right). Upper panels show the north-hemisphere summer season (June-July-August) and lower panels show the winter season (December-January-February). Blue dots mark positions where the N216 GLOMAP and EasyAerosol means are significantly different.*

Figure 4.5 shows the transect mean of precipitation rate for the summer and winter season. The blue dots mark where there is a significant difference between the GLOMAP and EasyAerosol N216 versions. Figure 4.5 shows that the spread between the different model versions in the mean precipitation rate along the transect is small. However, the spread is more prominent when the median precipitation rate is considered. Generally, and in both seasons, the high-resolution model version has a lower median rain rate than the low-resolution version. There is also a difference between the N216 GLOMAP and EasyAerosol simulations, where the JJA median is clearly higher for the GLOMAP version while in DJF the difference is very small.

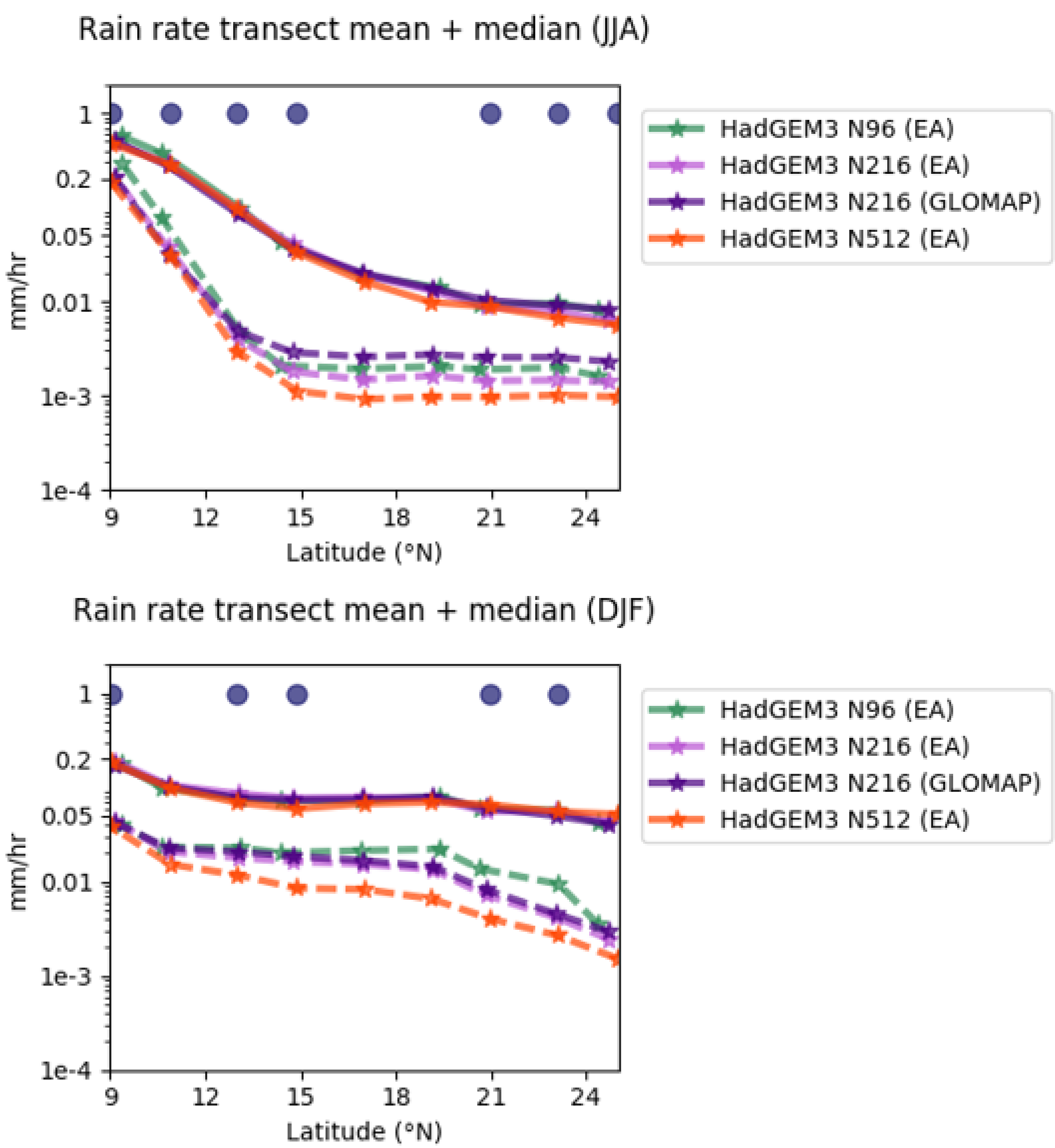

Figure 4.5: *Transect mean (solid) and median (dashed) of rain rate for JJA (upper panel) and DJF (lower panel). Blue dots mark positions where the N216-GLOMAP and N216-EasyAerosol (EA) means are significantly different.*

Figure 4.6 shows the frequency of rain events along the transect using 3-hourly model output integrated over a 6-hour time frame. Because most GCMs precipitate at least a little bit at virtually all time-steps, it was necessary to choose a limit where the precipitation rate is small enough to be negligible and considered a non-rain event. We calculate the statistics of rain events along the transect for different choices of such thresholds. The solid line displays the results for the lowest rain threshold of 10^{-4} mm hr^{-1}. In this case, all simulations precipitate at least 90% or more of all the times along the transect, and around 100% close to the deep convective region. The low-resolution version stands out with higher frequency of rain events in the mid-transect region in the summer season. With higher thresholds of negligible precipitation rates (0.001 mm hr^{-1} and 0.01 mm hr^{-1}), the model versions diverge clearly from each other along the transect. The high-resolution model has at least 10% higher frequency of rain events along the transect compared to the low-resolution model in the stratocumulus region, which is consistent with the transect mean and median results shown in Figure 4.5. The N216 GLOMAP version has more precipitating events than the

EasyAerosol version at the same resolution, and the differences are largest in summer. For the summer season the GLOMAP version stands out as the rainiest simulation in the stratocumulus region alongside with the low-resolution simulation.

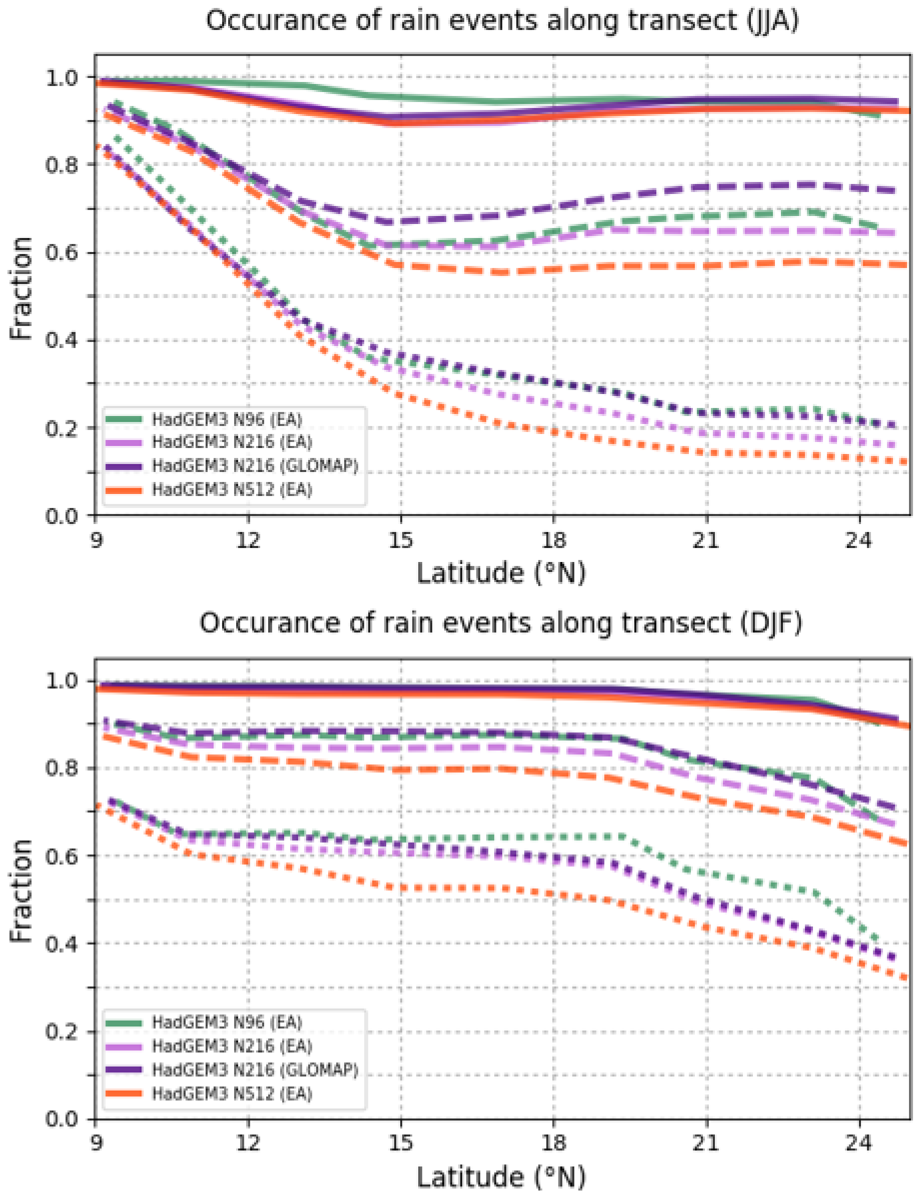

Figure 4.6: *Frequency of occurrence of rain events along the transect for three different lower thresholds to define a rain event: 10^{-4} mm hr^{-1} (solid), 0.001 mm hr^{-1} (dashed) and 0.01 mm hr^{-1} (dotted). Statistics based on 3-hour frequency output integrated over 6 hours.*

Figure 4.7 shows the probability distribution function (PDF) of rain rates for 3-hourly data for three different latitude regions, which each include two grid positions - i.e. there are two grid points representing the south-westerly deep convective region, two grid points representing the north-easterly stratocumulus region and two grid points representing the transition region at the middle of the transect. For the summer season, the GLOMAP medium resolution version has generally the highest rain rates in the stratocumulus region while the N512 simulation generally has the lowest rain rates, which is consistent with Figures 4.6 and 4.5.

In the mid transect region, the low and medium resolution simulation have a bimodal structure of rain rates with peaks at both 10^{-2} mm hr^{-1} and 10^{-4} mm hr^{-1}, while the high-resolution PDF is smoother and has a peak between the bimodal structure closer to 10^{-3}. The GLOMAP simulation has generally the highest rain rates in this mid-transect region, and they are higher than for the corresponding EasyAerosol simulation. In the convective region, the PDFs for the different versions do not differ as much as in the other regions. However, the low-resolution model version generally has a higher frequency of rain rates close to 1 mm hr^{-1} and the high-resolution version has a slightly higher peak at lower rain rates around 10^{-4} mm hr^{-1}. For the winter season the PDFs show basically the same structure as for JJA in the deep convective region. However, for the mid-transect and northerly regions the PDFs differ from the summer season. As seen in Figures 4.2 and 4.3 the SCT during winter is not as well defined which can be an explanation to the discrepancy in this season. Nevertheless, the low-resolution simulation has again generally higher rain rates and the high-resolution version have a slightly broader PDF and higher frequency of lower rain rates. Analogous to the summer season, the GLOMAP version have slightly higher rain rates than the corresponding EasyAerosol simulation.

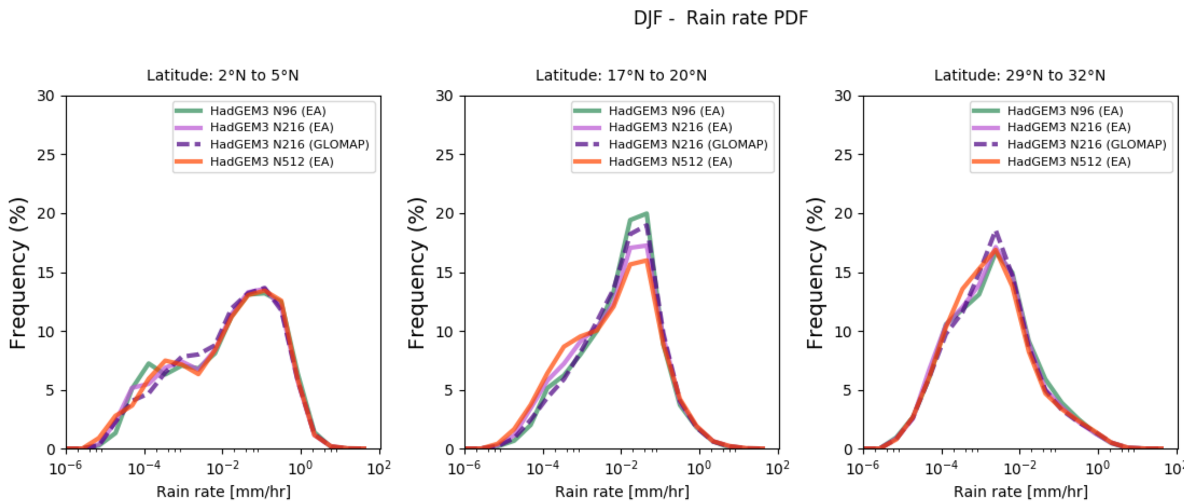

Figure 4.7: *Probability distribution function (PDF) of rain rates over three regions in the transect.*

Key points

- For the current model configuration, with prescribed SSTs and where the EasyAerosol version is based on output from the full-complexity aerosol model (GLOMAP), we find that neither model resolution nor the complexity of the aerosol scheme have a significant impact on the large-scale climatology of the stratocumulus to cumulus transition region along a North Eastern Atlantic transect. Very small and mostly non-significant differences are found in the dynamical setting of the transition and in the vertical distribution of liquid and ice water content.
- Model resolution and aerosol complexity do however have an impact on the integrated cloud water content and the precipitation rates along the transect.

- The low-resolution simulation has the highest water content especially in the convective region and more generally in the winter season. The low-resolution version also precipitates more frequently and generally has higher rain rates than the medium and high-resolution versions. The high-resolution version has the lowest frequency of rain events and the lowest rain rates along the transect. Discrepancies in rain rate probability distribution functions are found along the whole transect, but most notably in the stratocumulus and shallow cumulus regions.

- The GLOMAP version generally produces lower integrated liquid and ice water content than the corresponding simulation with EasyAerosol. It also rains more often, especially in the stratocumulus region. Furthermore, the GLOMAP simulation has the highest rain rates of all simulations in the stratocumulus and shallow cumulus regions.

3.5 Conclusion

WP3a scientists have compared multiple aspects of cloud, radiation, and aerosol distribution across different models, different horizontal resolutions, and different complexities of representation of aerosols and clouds. A good portion of the resolution/complexity space has been sampled, including documenting the impact of simplifying complexity to allow higher resolution models to be run reasonably quickly. The sensitivities to resolution and complexity for the simulations discussed in this document are summarised in Table 5.1.

Section	Variable	Sensitivity to resolution	Sensitivity to complexity
3.1	Radiative effect of aerosol-radiation interactions	N/A	Not sensitive. Simple prescriptions reproduce the radiative effects very well.
3.1	Radiative effect of aerosol-cloud interactions	N/A	Sensitive. Simple prescriptions need to account for temporal variability in cloud droplet number to reproduce the radiative effects.
3.1	Industrial-era aerosol effective radiative forcing	N/A	Sensitive. Simple prescriptions need to account for temporal variability in cloud droplet number to reproduce the radiative effects, although cancellations of biases between present-day and pre-industrial states decrease sensitivity.
3.2	Moisture flux into extratropical cyclones	Sensitive. Very high-resolution models required to match observations.	Sensitive. Complex cloud microphysics required for confidence in cloud response to aerosol changes and climate change.
3.2	Lightning flash rate	Sensitive. Low resolution models fail to simulate the diurnal cycle of convection correctly.	N/A
3.3	Cloud radiative effects	Not sensitive globally, although higher resolutions lead to regional improvements.	Sensitive to many physical parameterisations and process representations, initial conditions, and couplings between atmosphere and ocean.
3.4	Stratocumulus to cumulus transition in the Atlantic	Not sensitive in a large-scale sense, but cloud water content and rain rates are sensitive to resolution.	Not sensitive in a large-scale sense, but simple prescriptions of cloud droplet number concentrations produce thicker clouds and lower rain rates.

Table 5.1: *Summary of the findings of PRIMAVERA WP3a.*

It is of course possible that different model configurations would lead to different conclusions, but it is expected that the key conclusions listed in the Table 5.1 will remain valid qualitatively.

In terms of model development, the conclusions are reassuring for simulations that use simplified representations of aerosols. However, caution should still be exercised. Even if biases in present and pre-industrial conditions remain consistent, it is not known whether they would remain so in the future. In addition, even if radiative fluxes remain robust, that fact that changes in cloud water content have been identified may well lead to differences in future climate feedbacks. Repeating the analyses above with simulations set in different future climate would help quantifying whether climate feedbacks in models with simplified aerosol representations differ from those in more complex models.

There have been no sizeable deviations from the proposed work.

3.6 References

Caldwell, P.M., M.D. Zelinka, K.E. Taylor, and K. Marvel. Quantifying the Sources of Intermodel Spread in Equilibrium Climate Sensitivity. *J. Clim.*, 29(2): p. 513-524, https://doi.org/10.1175/JCLI-D-15-0352.1, 2016.

Edwards, J.M. and A. Slingo. Studies with a Flexible New Radiation Code. I: Choosing a Configuration for a Large-Scale Model. *Q. J. Ror. Meteor. Soc.*, 122, 689-71, http://dx.doi.org/10.1002/qj.49712253107, 1996.

Elsaesser, G.S., C.W. O'Dell, M.D. Lebsock, R. Bennartz, T.J. Greenwald, and F.J. Wentz. The Multisensor Advanced Climatology of Liquid Water Path (MAC-LWP). *J. Climate*, 30, 10193–10210, https://doi.org/10.1175/JCLI-D-16-0902.1, 2017.

Field, P.R., M.J. Roberts, and J.M. Wilkinson. Simulated Lightning in a Convection Permitting Global Model. J. Geophys. Res.: Atmospheres, 123(17), p. 9370-9377, https://doi.org/10.1029/2018JD029295, 2018.

Giorgetta, M. A., Brokopf, R., Crueger, T., Esch, M., Fiedler, S., Helmert, J., et al. ICON-A, the atmosphere component of the ICON Earth System Model. Part I: Model Description. *J. Adv. Model Earth Sy.*, 10, 1613–1637, https://doi.org/10.1029/2017MS001242, 2018.

Hill, A.A., B.J. Shipway, and I.A. Boutle. How sensitive are aerosol-precipitation interactions to the warm rain representation? *J. Adv. Model Earth Sy.*, 7(3), p. 987-1004, https://doi.org/10.1002/2014MS000422, 2015.

Kodama, C., et al. A 20-Year Climatology of a NICAM AMIP-Type Simulation. *J. Meteorol. Soc Jpn*, Ser. II, 93(4), p. 393-424, https://doi.org/10.2151/jmsj.2015-024, 2015.

Malavelle, F.F., et al. Strong constraints on aerosol–cloud interactions from volcanic eruptions. Nature, 546(7659), p. 485-491, https://doi.org/10.1038/nature22974 , 2017.

Manaster, A., C.W. O'Dell, and G. Elsaesser. Evaluation of Cloud Liquid Water Path Trends Using a Multidecadal Record of Passive Microwave Observations. *J. Clim.*, 30(15), p. 5871-5884, https://doi.org/10.1175/JCLI-D-16-0399.1, 2017.

Mann, G. W., K.S. Carslaw, D.V. Spracklen, D.A. Ridley, P.T. Manktelow, M.P. Chipperfield, S.J. Pickering, and C.E. Johnson. Description and evaluation of GLOMAP-mode: a modal global aerosol microphysics model for the UKCA composition-climate model, *Geosci. Model Dev.*, 3, 519-551, https://doi.org/10.5194/gmd-3-519-2010, 2010.

McCoy, D.T., et al. Mixed-phase cloud physics and Southern Ocean cloud feedback in climate models. *J. Geophys. Res.: Atmospheres*, 120(18), p.9539-9554, https://doi.org/10.1002/2015JD023603, 2015.

McCoy, D.T., et al. Aerosol midlatitude cyclone indirect effects in observations and high-resolution simulations. *Atmos. Chem. Phys.*, 18(8): p. 5821-5846, https://doi.org/10.5194/acp-18-5821-2018, 2018.

McCoy, D.T., et al. Cloud feedbacks in extratropical cyclones: insight from long-term satellite data and high-resolution global simulations. *Atmos. Chem. Phys. Discuss.*, https://doi.org/10.5194/acp-2018-785, in review, 2018.

Medeiros, B., C. Deser, R.A. Tomas, and J.E. Kay. Arctic Inversion Strength in Climate Models. *J. Climate*, 24, 4733–4740, https://doi.org/10.1175/2011JCLI3968.1, 2011.

Sandu, I., Stevens, B., and Pincus, R.: On the transitions in marine boundary layer cloudiness, *Atmos. Chem. Phys.*, 10, 2377-2391, https://doi.org/10.5194/acp-10-2377-2010, 2010.

Sato, Y., et al. Aerosol effects on cloud water amounts were successfully simulated by a global cloud-system resolving model. *Nature Communications*, 9(1): p. 985, https://doi.org/10.1038/s41467-018-03379-6, 2018.

Stevens, B., et al. MACv2-SP: a parameterization of anthropogenic aerosol optical properties and an associated Twomey effect for use in CMIP6. *Geosci. Model Dev.*, 10(1), 433-452, https://doi.org/10.5194/gmd-10-433-2017, 2018.

Taylor, J.P. and A. McHaffie. Measurements of Cloud Susceptibility. *J. Atmos. Sci.*, 51, 1298–1306, https://doi.org/10.1175/1520-0469(1994)051<1298:MOCS>2.0.CO;2, 1994.

Teixeira, J., S. Cardoso, M. Bonazzola, J. Cole, A. Del Genio, C. DeMott, C. Franklin, C. Hannay, C. Jakob, Y. Hiao, J. Karlsson, H. Kitagawa, M. Köhler, A. Kuwano-Hoshida, C. LeDrain, A. Lock, M.H. Miller, P. Marquet, J. Martins, C.R. Mechoso, E.V. Meijgaard, I. Meinke, A.M.A. Miranda, D. Mironov, R. Neggers, H.L. Pan, D.A. Randall, P.J. Rasch, B. Rockel, W.B. Rossow, B. Ritter, A.P. Siebesma, P. Soares, F.J. Turk, P.A. Vaillancourt, A. Von Engeln, and M. Zhao. Tropical and subtropical cloud transitions in weather and climate prediction models: the GCSS/WGNE Pacific Cross-section Intercomparison (GPCI). *J. Climate*, 24, 5223-5256, https://doi.org/10.1175/ 2011JCLI3672.1, 2011.

Wilson, D. R., et al. PC2: A prognostic cloud fraction and condensation scheme. I: Scheme description. *Q. J. Ror. Meteor. Soc.*, 134(637), 2093-2107, 2008.

Woods, C., R. Caballero, and G. Svensson. Representation of Arctic Moist Intrusions in CMIP5 Models and Implications for Winter Climate Biases. *J. Climate*, 30, 4083–4102, https://doi.org/10.1175/JCLI-D-16-0710.1, 2017.

Yoon, J-H., P. Rasch, S. Ghan, B. Singh, B. Eaton, F. Vitt, H. Wang, and K. Zhang. A “final” version of prescribed aerosols for CAM5' - Presentation to the Atmosphere Model Working Group (AMWG), Community Earth System Model, 2013

3.7 Peer-reviewed WP3a articles

Submitted or accepted

McCoy, D. T., Field, P. R., Schmidt, A., Grosvenor, D. P., Bender, F. A. M., Shipway, B. J., Hill, A. A.; Wilkinson, J. M., Elsaesser, G. S., 2018: Aerosol midlatitude cyclone indirect effects in observations and high-resolution simulations. *Atmos. Chem. Phys.*, https://doi.org/10.5194/acp-18-5821-2018.

McCoy, D. T., Bender, F. A-M., Grosvenor, D. P., Mohrmann, J. K., Hartmann, D. L., Wood, R., Field, P. R., 2018: Predicting decadal trends in cloud droplet number concentration using reanalysis and satellite data. Atmos. Chem. Phys., doi: https://doi.org/10.5194/acp-18-2035-2018.

Thomas, M. A., A. Devasthale, T. Koenigk, K. Wyser, M. Roberts, C. Roberts, K. Lohmann, 2018: A statistical and process-oriented evaluation of cloud radiative effects in high resolution global models. Geophys. Model Dev. Discuss., *submitted*.

In preparation

Nygren, E., Ekman A. M. L., Bellouin, N. Impact of spatial resolution and aerosol scheme complexity on simulations of stratocumulus to cumulus transition in a global climate model, *in preparation*, 2019.

4. Lessons Learnt

Nothing specific to report.

5. Links Built

WP3a scientists have worked with WP6 to implement EasyAerosol in HadGEM3. In return, WP6 contributed the additional EasyAerosol simulations analysed in Sections 3.1 and 3.4.